

**Revista Mexicana de
Astronomía y Astrofísica**

Revista Mexicana de Astronomía y Astrofísica

ISSN: 0185-1101

rmaa@astroscu.unam.mx

Instituto de Astronomía

México

Retes, R.; Luna, A.; Mayya, Y. D.; Carrasco, L.
EMBEDDED YOUNG STELLAR POPULATION IN THE GALACTIC MOLECULAR CLOUD
ASSOCIATED WITH IRAS 18236-1205

Revista Mexicana de Astronomía y Astrofísica, vol. 37, 2009, pp. 165-169

Instituto de Astronomía

Distrito Federal, México

Available in: <http://www.redalyc.org/articulo.oa?id=57115687027>

- How to cite
- Complete issue
- More information about this article
- Journal's homepage in redalyc.org

redalyc.org

Scientific Information System

Network of Scientific Journals from Latin America, the Caribbean, Spain and Portugal

Non-profit academic project, developed under the open access initiative

EMBEDDED YOUNG STELLAR POPULATION IN THE GALACTIC MOLECULAR CLOUD ASSOCIATED WITH IRAS 18236-1205

R. Retes,^{1,2} A. Luna,¹ Y. D. Mayya,¹ and L. Carrasco¹

RESUMEN

Presentamos un estudio de la nube molecular asociada con la fuente IRAS 18236-1205 para identificar su población joven estelar embebida. Para la selección de estos objetos, hemos usado un criterio geométrico basado en los contornos de intensidad del gas molecular ^{13}CO del *Galactic Ring Survey (GRS)*, además de criterios fotométricos basados en datos del cercano infrarrojo 2MASS. Con esta selección hemos encontrado dos objetos asociados a la fuente IRAS. Sus distribuciones espectrales de energía (*SEDs*) en el rango espectral del cercano al lejano infrarrojo fueron modelados como la suma de flujos de un objeto estelar de tipo espectral temprano enrojecido más una envolvente de polvo. Del ajuste realizado, hemos obtenido dos objetos tempranos de tipo espectral B0.5V y B8V para los objetos asociados a la posición de la fuente IRAS. Estos pueden ser responsables de la emisión IRAS observada de 60 a 100 μm . Un objeto no identificado por 2MASS fué encontrado usando datos de IRAC-SPITZER. Este objeto se encuentra asociado a un arco con emisión a 4.5 μm , sugiriendo la presencia de un *outflow*.

ABSTRACT

We study the molecular cloud associated with the ultracompact HII region IRAS 18236-1205 to identify the young stellar objects (YSOs) embedded in the cloud. The ^{13}CO intensity contours from the Galactic Ring Survey (GRS) data were used to define the geometry of the cloud, and the search for YSOs was carried out based on the NIR 2MASS photometric data. The search yielded two objects inside the IRAS beam, both with counterparts with the recently available *Spitzer sources*. The NIR to FIR Spectral Energy Distributions of these two sources were modeled as the sum of fluxes of an embedded hot star and a warm dust envelope. From the resulting fits, we infer spectral types of B0.5V and B8V for the two YSOs, both experiencing visual extinctions of ~ 20 mag, with the former source responsible for almost all the observed emission in the IRAS 60 and 100 μm bands. A third stellar object inside the IRAS beam was identified only on the *Spitzer* images, and is associated with an arc at 4.5 μm , which we propose as a low-mass star with an outflow.

Key Words: HII regions — ISM: clouds — stars: formation — stars: Pre-main sequence

1. THE MOLECULAR CLOUD ASSOCIATED TO IRAS 18236-1205

The IRAS 18236-1205 source have typical IRAS colors of UCHII regions (Wood & Churchwell 1989), and is associated with the OH and H_2O maser emission, in addition to the high density tracer CS(J=2 \rightarrow 1) emission (Bronfman et al. 1996). These features make this region a good candidate of massive star forming region. However, the source is yet to be investigated to identify their embedded stellar populations.

We selected and defined the molecular cloud towards IRAS 18236-1205 source using the ^{13}CO data of the Galactic Ring Survey (Jackson et al. 2006). We used a 24×24 arcmin field centered at IRAS po-

sition within the velocity range of 18–32 km s^{-1} , suggested by the CS(J=2 \rightarrow 1) emission (Bronfman et al. 1996). The ^{13}CO integrated emission is showed in the Figure 1. The geometry of the region is elongated and inclined with respect to the galactic plane, and shows a central structure of higher emission with substructures of emission along the cloud. The position of the IRAS source is indicated in Figure 1 with a white star symbol. From analysis of the ^{13}CO molecular gas, we have obtained physical parameters of the molecular cloud, which are listed in Table 1.

2. THE SELECTION OF STELLAR POPULATION

The study of the stellar component was made using the J, H, K_S photometry in the Point Source Catalog (PSC) of 2MASS (Skrutskie et al. 2006). We selected sources on a 24×24 arcmin field centered on the IRAS source. Only point sources (PS) with

¹Instituto Nacional de Astrofísica Óptica y Electrónica, Apdo. Postal 51 y 216, Puebla, México (rretes@inaoep.mx).

²This work is based on the results of INAOE MSc-Thesis of the author.

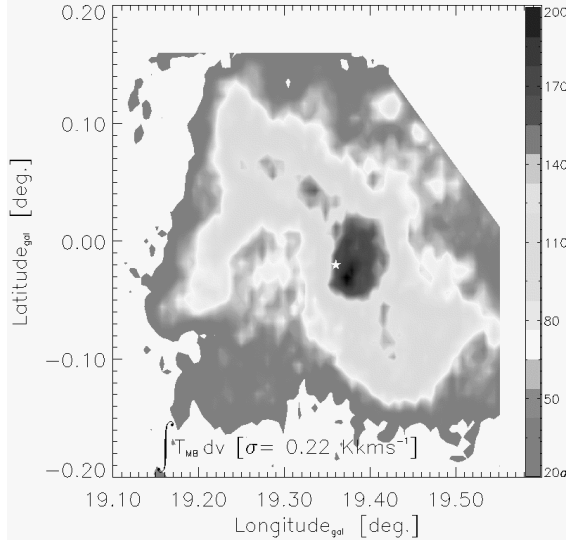


Fig. 1. ^{13}CO intensity map of the molecular cloud associated with IRAS 18236-1205. The map is obtained by integrating the CO intensities in the velocity range 18–32 km s $^{-1}$, which covers all the velocity channels associated with the cloud.

TABLE 1

PHYSICAL PARAMETERS CALCULATED FOR THE MOLECULAR CLOUD ASSOCIATED TO IRAS 18236-1205

| Parameter | Value [Unity] |
|----------------------|------------------------------------|
| T_K | 22.5 [K] |
| τ^{13} | 0.74 |
| τ^{12} | 42.2 |
| $N(^{13}\text{CO})$ | 9.7×10^{16} [cm $^{-2}$] |
| $N(\text{H}_2)$ | 4.8×10^{22} [cm $^{-2}$] |
| A_V | $\gtrsim 30$ [mag] |
| Velocity (peak) | 26.35 [km s $^{-1}$] |
| FWHM | 4.90 [km s $^{-1}$] |
| Distance (kinematic) | 2.42 [kpc] |
| M_{VIR} | 1.5×10^4 [M_\odot] |
| M_{LTE} | 5.0×10^4 [M_\odot] |

good photometry in the K_S band, and inside the 40σ contour level area of ^{13}CO velocity-integrated emission were used (Figure 1). This was our first selection criteria and we will call this subset PS Filter 1. Subset PS Filter 1 was plotted on the $J - H$ vs. $H - K_S$ color-color diagram (Figure 2). It can be seen that the reddened main sequence stars occupy a very small band in this diagram, with majority of

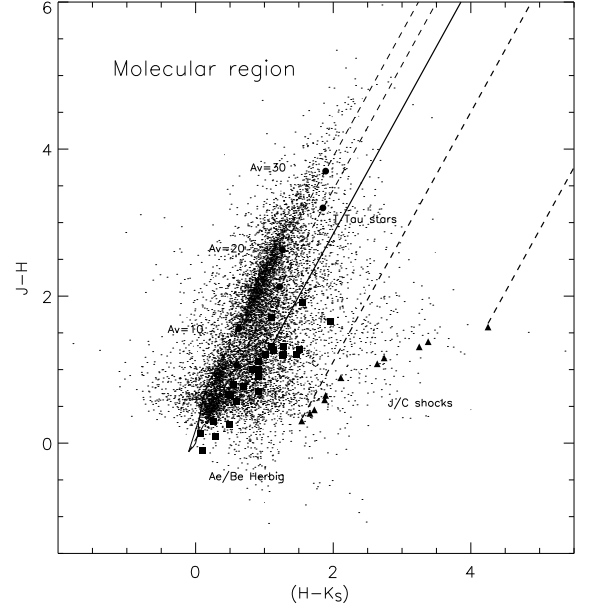


Fig. 2. Color-color diagram ($J - H$) vs. ($H - K_S$) of the 2MASS point sources (dots) in the area delimited by the ^{13}CO emission. Tracks for Main Sequence and Giants are shown with solid lines ($0 < H - K_S < 0.5$ and $0 < J - H < 1$). Effect of reddening these tracks is shown by the dashed lines, with the position of visual extinctions of 10, 20 and 30 mag shown. The expected position of the Pre-Main Sequence objects are also shown: T-Tauri stars along with the reddening vector (solid line starting at $H - K_S = 1.0$ and $J - H = 1$), Ae/Be stars (solid squares), and shocked objects associated with HH objects (solid triangles, with reddening vectors shown in dashed lines for the two extreme color objects).

sources showing an excess in the $H - K_S$ color. From the figure it is easy to see that these sources with a color excess are objects related with earlier phases of stellar evolution (Lada & Adams 1992; Roman-Lopes & Abraham 2006). In rest of our analysis, we use only these sources.

Some of the sources selected in subset PS Filter 1 may be foreground/background objects and hence may not be embedded in the cloud. These sources were filtered out by analyzing the photometry of stars in a control field. The ($H - K_S$) histogram for the subset PS Filter 1 (solid line) is compared to that for a control region (dotted line) in Figure 3. The control region was selected with the same size as that of the object field, centred on galactic coordinates (19.40, -1.85). We note a single mode distribution for the control region and a bimodal distribution for the molecular region. The maximum value

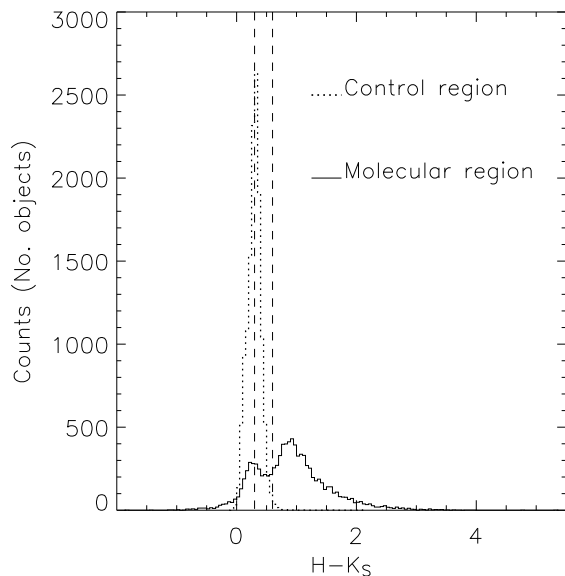


Fig. 3. Color ($H - K_S$) histograms of 2MASS sources associated with the molecular cloud and a control region.

of the bluer component of the bimodal distribution (molecular region) is coincident with the maximum value for the control histogram which is shown by the dashed line. We interpret this bluer component as due to the foreground stars.

3. IDENTIFICATION OF EMBEDDED YSOS FROM 2MASS DATA

The Young Stellar Objects (YSOs) are in their early phase of evolution and are expected to occupy the region corresponding to the pre-main sequence objects in the $J - H$ vs $H - K_S$ diagram. From Figure 2, we can see that there are plenty of stars in this region which are all potential candidates. The reddest of these stars are the best candidates for being embedded YSOs. In this study, we limit our analysis to the sources that have $H - K_S > 2.5$, and geometrically placed in the molecular region (limited by ^{13}CO). This is our second filter (Filter 2) and final criterion of selection. These sources are shown in the K_S vs. ($H - K_S$) color-magnitude (CM) diagram in Figure 4. The NIR excess of these objects could be due to circumstellar disks and/or emission of dusty envelopes, typical of YSOs embedded in their parent molecular clouds (Lada & Adams 1992). Due to the fact that the molecular region presents high columnar density (§ 1), we do not expect to see the stars localized beyond of the molecular region (background star field).

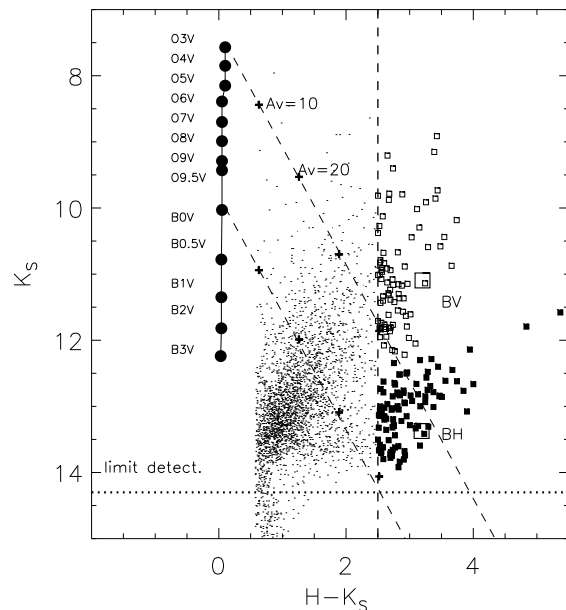


Fig. 4. Color-magnitude diagram of the embedded sources. Sources with $H - K_S < 1.5$ CM diagram with the VBOs and HBOs objects selected into the molecular cloud. See explanation in text.

In this figure, we can see a tendency for the relatively fainter stars to be statistically more redder than the K_S bright objects. Hence, tentatively we divide the objects selected with last photometric criterion (Filter 2) into two groups: horizontal branch objects (HBOs, filled squares) and vertical branch objects (VBOs, open squares). Two of these objects are located inside the IRAS beam, which are indicated by a square symbol in Figure 4, followed by labels BV and BH. We searched in the PSC *IRAC-SPITZER* objects that are within $0.5''$ from the position of the 2MASS sources, and found *IRAC-SPITZER* counterparts for both BV and BH. A third source was identified with IRAC data within the IRAS beam without any 2MASS counterpart, which we name as OCII object. In the following, we investigate whether these are responsible for the observed emission in the IRAS bands. In order to do this, we look at their multi-band spectral energy distributions.

4. SPECTRAL ENERGY DISTRIBUTION (SED) OF YSOS ASSOCIATED WITH IRAS 18236-1295

The spectral distribution energy (SED) of sources in the IRAS beam (~ 1 arcmin) was used to analyse why the IRAS source has typical colors of UCHII region. Two sources in the beam were found, one

HOB object and one VBO object. A third source identified with IRAC data (OCII object; Allen et al. 2004) was found also in the IRAS beam. We constructed a simple model to explain the observed SEDs of these sources. The model consists of two sources of emission: (1) an embedded star, whose ultraviolet-optical radiation is absorbed by the dust surrounding the star, and (2) warm dust, which re-radiates all the absorbed energy in the IRAS bands. The SEDs of these two components are calculated using the formulas:

$$F_{\lambda}^* = \left(\frac{R_{\star}}{D}\right)^2 c_1 \pi B_{\lambda}(T_{\text{eff}}) e^{-\tau_{\lambda}}, \quad (1)$$

and,

$$F_{\lambda,\text{env}}^{\text{warm}} = \frac{A_{\text{warm}}}{4\pi D^2} c_1 B_{\lambda}(T_{d,\text{warm}})(1 - e^{-\tau_{\lambda}}), \quad (2)$$

respectively.

The fit to observational data is given by the expression,

$$\log [\lambda F_{\lambda}(\text{Obs})] \simeq \log [\lambda F_{\lambda}^* + \lambda F_{\lambda,\text{env}}^{\text{warm}}], \quad (3)$$

where R_{\star} and T_{eff} are the stellar radius and effective temperature, respectively. Their values are obtained from Cox (2000) and Hanson et al. (1997). The adopted distance is $D=2.5$ kpc (Bronfman et al. 1996), c_1 is a constant. The dust temperature ($T_{d,\text{warm}}=26\text{K}$) for the envelope is according to estimation by Faúndez et al. (2004). The fit parameter A is related to projected area of dust circumstellar envelope, and calculated with the expression $A_{\text{warm}} = L_{\text{bol}}/\sigma T_d^4$. The emission of the warm dusty envelope is related with each spectral type through the A factor, described above. We have used a Cardelli extinction curve.

The Black-Body (BB) emission in each case must fit the observational 2MASS NIR data (stellar component) and it is limited by the spectral type of star associated to IRAS luminosity (B0.5V). So, the corresponding spectral type for the VB object are B0.5V, with a visual extinction value of 21 mag (Figure 5, top). This source has enough ionizing radiation to create the UCHII region fluxes observed by IRAS. A spectral type of B8V for the HB object and F0V for the OCII object have better (visual) fitting, both with a extinction value of 20 mag. (Figure 5, middle and bottom panels). In the OCII case, a third hot component was necessary which is probably associated with an envelope or circumstellar disk immediately surrounding the star. This component is calculated using the expression:

$$F_{\lambda,\text{env}}^{\text{hot}} = \frac{A_{\text{hot}}}{4\pi D^2} c_1 B_{\lambda}(T_{d,\text{hot}})(1 - e^{-\tau_{\lambda}}), \quad (4)$$

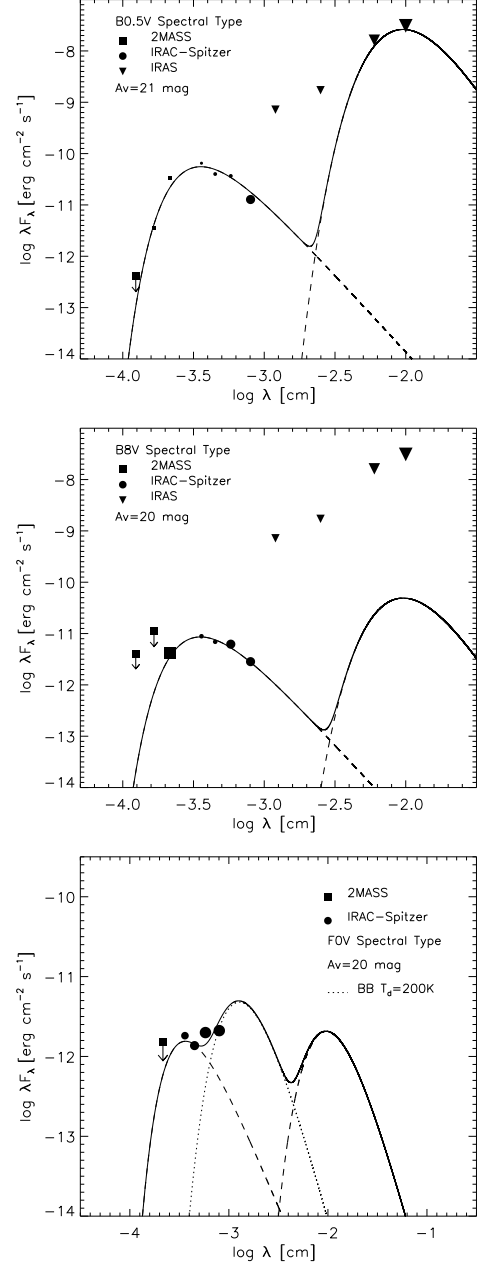


Fig. 5. SED for the objects in the IRAS beam: VBO (top), HBO (middle) and CHIO (bottom). The stellar and warm dust components are plotted with dashed lines. The sum of components is plotted with solid line. The sizes of the data symbols are proportional to error on the data, and data with upper limits are plotted with downward pointing arrows. All the three sources are inside the IRAS beam. These fits illustrate that the entire observed IRAS flux comes from the first source (VBO), which is a main sequence star of spectral type B0.5V.

given by a “hot” dusty envelope (Figure 5, bottom, dotted line), with a temperature $T_{d,hot}=200\text{K}$. In Figure 5 (bottom), this hot component is shown by the dotted line and reproduces fairly well the observed fluxes in the Spitzer/IRAC bands. However, we note that the emission in this region of the spectrum comes from heating of the PAHs, whose emission spectrum resembles more a power-law spectrum rather than the Black Body approximation we have used. In a forthcoming paper, we will make a more detailed analysis of this part of the spectrum. The value of the parameter A_{hot} is equal to $0.1 A_{warm}$. In this case, The fit to observacional data is given by the expression,

$$\log [\lambda F_{\lambda}(\text{Obs})] \simeq \log [\lambda F_{\lambda}^* + \lambda F_{\lambda,env}^{warm} + \lambda F_{\lambda,env}^{hot}] \quad (5)$$

this improved model is in agreement with low mass object with a disk (T Tauri star?).

5. CONCLUSIONS

We present a method for selection of embedded YSOs in the molecular cloud towards IRAS 18236-1205 source. The embedded young stellar population was defined using two criteria to filter them: one geometrical criterion based on ^{13}CO data, and the other one based on NIR 2MASS photometric data. With this method we have selected a set of objects with high $(H-K_S)$ excess. Spatially, these objects are associated with densest structures of the molecular cloud. The SED of two selected objects associated to IRAS source and inside the IRAS beam were modelled in acceptable agreement to photometric data.

The stellar spectral type associated to each object is B0.5V and B8V, both experiencing around 20–21 magnitude of visual extinction. The first of these stellar objects have enough ionizing radiation to create the UCHII region fluxes observed by IRAS. A third object was found in the IRAS beam, on the Spitzer/IRAC images with no detection in 2MASS. The proposed spectral type for this object is F0V, and is associated with an extended emission at $4.5 \mu\text{m}$. The extended emission at $4.5 \mu\text{m}$ is usually due to shocked gas, which suggest the presence of an outflow (HH object?) associated with this third source.

This work is based on ^{13}CO data of GRS (Boston Univ. & FCRAO), images and PSC data of 2MASS (UMASS & IPAC-JPL-CalTech), and images and PSC data from IRAC-Spitzer (Spitzer ST/JPL-CalTech). Part of this work was done with the CONACYT fellowship 199493 of first author.

REFERENCES

- Allen, L. E., et al. 2004, ApJ, 154, 363
 Bronfman, L., Nyman, L.-Å, & May, J. 1996, A&AS, 115, 81
 Cox, A. N. 2000, Allen’s Astrophysical Quantities (Melville: AIP)
 Faúndez, S., et al. 2004, A&A, 426, 97
 Jackson, J. M., et al. 2006, ApJ, 163, 145
 Lada, C. J., & Adams, F. C. 1992, ApJ, 393, 278
 Retes, R. 2008, MsC thesis, INAOE, Mexico
 Roman-Lopes, A., & Abraham, Z. 2006, A&A, 471, 813
 Skrutskie, M. F., et al. 2006, AJ, 131, 1163
 Wood, D. O. S., & Churchwell, E. 1989, ApJ, 340, 265